Polymer 50 (2009) 2113–2122

Contents lists available at ScienceDirect

Polymer

journal homepage: www.elsevier.com/locate/polymer

Micro-patterned polystyrene surfaces directed by surfactant-encapsulated polyoxometalate complex via breath figures

Hang Sun, Haolong Li, Lixin Wu*

State Key Laboratory of Supramolecular Structure and Materials, Jilin University, Qianjin Street 2699, Changchun 130012, PR China

ARTICLE INFO

Article history:
Received 9 October 2008
Accepted 15 February 2009
Available online 28 February 2009

Keywords:
Polystyrene
Polyoxometalate
Honeycomb-patterned microporous film

ABSTRACT

In this paper, surfactant-encapsulated polyoxometalate complex, $(DODA)_9[EuW_{10}O_{36}]$ (SEC-1), is applied to functionalize the breath figure holes of polystyrene (PS) film via a straightforward, one-step process by doping SEC-1 into PS solution. Accompanied with the self-organization of the water droplets, amphiphilic SEC-1 is found to self-assemble at the PS solution–water droplet interface to stabilize the water droplets, and it effectively enhances the order of the PS microporous film. Highly ordered PS microporous film in which SEC-1 accumulates on the internal surfaces of the holes with an ordered and tight lamellar structure was obtained. The film exhibits intense red emission under ultraviolet light excitation deriving from SEC-1. Ag and Fe_2O_3 nanoparticles have been successfully introduced into the microporous structure through different ways. This new method is also suitable for other polymers, and the polyoxometalates with applicable properties could be readily applied to functionalize the holes of polymer microporous films.

1. Introduction

Ordered microporous polymer surfaces have attracted considerable attention over recent years for their potential applications in patterned templates, membranes, photonic or optoelectronic devices, catalysis, sensors, and so on [1]. Among those techniques for the fabrication of honeycomb structured films, the breath figure is proved to be an effective dynamic template method through providing a humid condition to the surface of polymer solution in a volatile solvent and has been extensively applied because of its facility, speediness and economy [2]. The condensed water droplets caused by rapid cooling due to solvent evaporation self-organize into a well ordered hexagonal array that acts as the template directing the formation of ordered microporous structure [3]. By using this method, a variety of materials such as linear [4], starlike [2,5], block [6], amphiphilic [7], and conjugated polymers [8], even surface modified nanoparticles [9], have been successfully employed for the fabrication of ordered microporous films. Among those polymers, polystyrene (PS) as a representative of commodity polymers, has been extensively investigated for the pattern formation based on the interests in both fundamental research and practical application [4,10]. However, PS itself is difficult to form ordered microporous film generally because of its poor hydrophilicity, unless the molecular weight of PS and the preparation conditions are strictly controlled [10]. Furthermore, PS possesses only a small range of refractive indices, and it is electrically insulating, nonmagnetic, nonluminous and chemically unreactive, which greatly limits the application of the PS microporous film. It is noted that the adsorption of suspended particles with micrometer and nanometer size at the interface between immiscible liquids has been described previously [11]. In the case of breath figure formation from a polymer solution, the interface between the polymer solution and the water droplets could serve as the template for the self-assembling of amphiphilic molecules and nanoparticles, which provides an opportunity to enhance the order of the polymer microporous film and to functionalize the holes. And, the combination of the self-organized and self-assembly processes on different length scales may lead to novel hierarchical structures with special functions. Both topologically and chemically heterogeneous patterns have been obtained in amphiphilic block copolymer and nanoparticle/polymer mixed systems, which exhibit potential applications in sensor, microreactor and catalysis [6b,12].

Polyoxometalates (POMs) are intriguing nanosized clusters with a variety of applicable properties such as catalysis, redox, optics and electrochemistry [13]. To perform these functions in organized systems, POMs have been modified by replacing their counterions with cationic surfactants [14a]. The formed amphiphilic surfactant-encapsulated clusters (SECs) possess a hydrophobic shell of alkyl chain and a hydrophilic core of cluster, and have been proved to be

* Corresponding author. Tel.: +86 431 85168481; fax: +86 431 85193421.
E-mail address: wulx@jlu.edu.cn (L. Wu).

0032-3861/$ – see front matter © 2009 Elsevier Ltd. All rights reserved.
doi:10.1016/j.polymer.2009.02.036

promising building blocks because the physical and chemical properties of POMs are well kept in organized assemblies [14]. It is noted that the ordered assembling of SECs yields a new route to control their structural, electronic, optical and catalysis properties. However, the periodic structure of SECs has been rarely reported. To obtain SECs based ordered surface structure, recently, we have reported that some SECs with proper wettability could form ordered microporous structures via breath figures [15]. As a further insight, the aim here is to functionalize the breath figure holes of the PS microporous film in a straightforward, one-step process through the site-controlled self-assembling of SECs at the PS solution–water droplet interface during the self-organization of the water droplets, and obtain novel hybrid film with hierarchically structure and synergetic property. In addition, we expect that the SECs self-assembling at the interface could stabilize the water droplets effectively, which could enhance the order of the PS microporous film in a much larger scale.

Therefore, in this paper, we demonstrated the use of a typical photoluminescent complex that was well characterized previously, $(DODA)_9(EuW_{10}O_{36})$ (SEC-1, DODA denotes dimethyl dioctadecylammonium, $EuW_{10}O_{36}$ represents inorganic polyanion cluster $[EuW_{10}O_{36}]^{9-}$ and is abbreviated as POM-1), to functionalize the breath figure holes in PS film by doping SEC-1 into PS solution [14b]. The results show interesting features of the combination of the self-organized and self-assembly processes on different length scales in polymer/SECs mixed system: The chemical structure and physical properties of SEC-1 are well maintained in PS microporous film; The doped SEC-1 effectively stabilizes water droplets and enhances the order of the PS microporous film, forming highly ordered hybrid microporous structure in a large scale; SEC-1 accumulates along the internal surfaces of the holes with an ordered and tight lamellar structure in PS microporous film through microphase separation. Furthermore, Ag and Fe_2O_3 nanoparticles have been successfully introduced into the ordered microporous structure by different methods, depending on the obtained SECs functionalized microporous film. The present research draws an effective route to fabricate highly ordered microarrays of SECs functionalized holes in polymer matrix, revealing potential applications in sensor, microreactor and catalysis.

2. Experimental section

2.1. Materials

PS ($M_w = 349\ kg\ mol^{-1}$) and dimethyl dioctadecylammonium bromide (DODA·Br, 99%) were purchased from Acros Organics and used as received. $Na_9[EuW_{10}O_{36}]$ (POM-1) and $K_{12}[EuP_5W_{30}O_{110}]$ (POM-2) were freshly prepared according to the literature procedures, respectively [14f,14g]. $(DODA)_9[EuW_{10}O_{36}]$ (SEC-1) and $(DOAH)_{12}[EuP_5W_{30}O_{110}]$ (SEC-2) (DOAH: dioctadecylammonium hydrobromide) were synthesized following our published work [14b]. Octylamine-protected Fe_2O_3 nanoparticles (average diameter: 5.7 nm) were synthesized according to a published procedure (see Supporting information).

2.2. Preparation of microporous films

We have prepared the chloroform solutions of PS (6 mg/mL), SEC-1 (5 mg/mL), PS (6 mg/mL) containing different concentrations of SEC-1 (0.03, 0.06, 0.12, 0.25, 0.32, 1, 2, and 6 mg/mL), as well as containing DODA (1 mg/mL), respectively. The microporous thin films were prepared by direct casting 20 μL of sample solutions onto glass substrates under a moist airflow at ambient temperature. The humid condition was achieved by bubbling nitrogen gas through a water-filled conical flask, and then the nitrogen gas saturated with water vapor was sent from a glass nozzle onto the surface of sample solution.

2.3. Measurements

The optical photographs were taken with an Olympus BX-51 optical microscope (OM). Scanning electron microscopy (SEM) images were collected on a JEOL JSM-6700F field emission scanning electron microscope. Atomic force microscopy (AFM) images were carried out with a commercial instrument (Digital Instrument, Nanoscope III, and Dimension 3000™) at room temperature in air. Transmission electron microscopy (TEM) images were obtained with a JEOL-2010 electron microscope operating at 200 kV. X-ray diffraction was performed on a Rigaku X-ray diffractometer (D/max rA, using Cu Kα radiation at a wavelength of 1.542 Å), and the data were collected from 0.7 to 10°. Luminescence measurements were performed on a HITACHI F-4500 Fluorescence spectrophotometer. Thermogravimetric analysis (TGA) was conducted with a Perkin–Elmer TG/DTA-7 instrument and the heating rate was 10 K/min. Magnetic force microscopy (MFM) image was carried out with a commercial instrument (NT-MDT Solver P47 Pro) using NSG01/Co needlepoint.

3. Results and discussion

3.1. Honeycomb-patterned hybrid PS film doped with SEC-1

To obtain highly ordered breath figure holes for SEC-1 self-assembling, we have investigated the influence of the doped SEC-1 on the morphology of the PS microporous film to optimize the preparation condition. The optical micrographs in Fig. 1 show the patterned surfaces of PS, SEC-1, and their mixture, prepared by casting their chloroform solutions onto glass substrates under the same humid condition, respectively. For pure PS ($M_w = 349\ kg\ mol^{-1}$) film prepared by casting its solution of 6 mg/mL, large disordered holes with a relatively broad size distribution (some of which are even close to 40 μm) are observed everywhere in the casting field due to the coagulation of the water droplets (Fig. 1a). Similar large disordered holes were observed for the concentrations of PS solution ranging from 1 to 20 mg/mL. The poor hydrophilicity of PS is unfavorable for the stabilization of water droplets, which should be responsible for the disordered morphology, and the similar results have been reported by several other groups [3c,5,10b]. In the case of SEC-1 (5 mg/mL), it can stabilize water droplets efficiently as mentioned in our previous work, and its corresponding film shows an ordered honeycomb structure with occasional defects (Fig. 1b) [15b]. The ordered honeycomb structure could be kept in a large concentration range of the solution from 0.5 mg/mL to 10 mg/mL. In contrast to pure PS, for the mixed solution of PS (6 mg/mL) doped with SEC-1 (1 mg/mL), highly ordered honeycomb-patterned film showing monodispersed hexagonal close-packed holes with a long range order forms in a large area without defects (approximate $200 \times 150\ \mu m^2$) as seen in Fig. 1c. From these results it is known that the doped SEC-1 efficiently stabilizes water droplets and prevents them from coagulation, which apparently enhances the order of the microporous film, forming highly ordered honeycomb-patterned hybrid PS film. The good processibility of PS makes the mixture easily processed into thin film, and compared with pure SEC-1, the mixed film shows more homogeneous hole size as well as more ordered hole arrangement.

We investigated the influence of the amount of the doped SEC-1 on the morphology of the formed PS microporous film in detail. From the corresponding optical micrographs in Fig. 2, it can be clearly seen that with increasing the amount of doped SEC-1 from 0.03 mg/mL to 0.06 mg/mL, then to 0.12 mg/mL, both the average

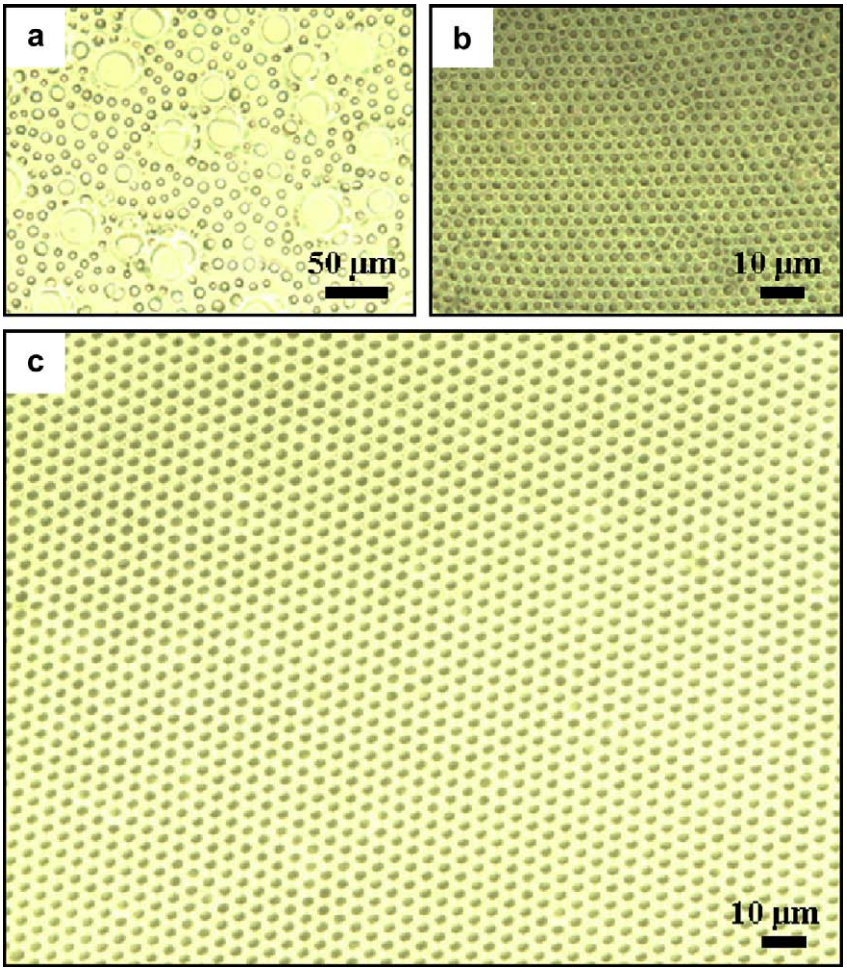

Fig. 1. Optical micrographs of patterned surfaces casting from (a) 6 mg/mL of PS, (b) 5 mg/mL of SEC-1, and (c) 6 mg/mL of PS containing 1 mg/mL of SEC-1, respectively.

size and the size distribution of the holes decrease markedly, together with the arrangement of the holes becomes ordered gradually, indicating the effective inhibition of SEC-1 for the coagulation of water droplets. With the further addition of SEC-1 (up to 0.25 mg/mL), the arrangement of the holes becomes more ordered and the hole size changes little, but the visible defects still exist. When the additive SEC-1 reaches 0.32 mg/mL (5 wt%), highly ordered honeycomb-patterned PS film is obtained in a relatively large area which cannot be achieved for pure SEC-1 film. This demonstrates that SEC-1 owns highly stable efficacy to water droplets and can induce PS to form ordered honeycomb structure efficiently. The highly ordered honeycomb structures are well kept until the amount of doped SEC-1 increases up to 2 mg/mL. The pattern of the mixed film tends to the case of pure SEC-1 with further increasing the content of addictive SEC-1 to 6 mg/mL. Namely, the quality of the hybrid microporous film decreases accompanied with the appearance of a few defects. Combining the processibility of PS and the stability of SEC-1 to the water droplets, highly ordered honeycomb structures could be prepared through the proper doping of SEC-1 to PS.

It is known that some surfactant molecules could be used as the stabilizer of emulsion through adsorbing at liquid–liquid interface [16]. As a kind of amphiphilic complex, SEC-1 is nanosized and owns large molecular weight (7526 g mol^{-1}), which is different from conventional surfactant molecules. To evaluate the contribution of SEC-1 for the pattern formation, we employed pure DODA ($M_w = 631$ g mol^{-1}), which was used for the encapsulation of POM-1, to mix with the chloroform solution of 6 mg/mL of PS for the control experiment. When the content of doped DODA is 1 mg/mL, poorly ordered microporous film is obtained as shown in Fig. 2h, and the size distribution of holes is relatively broad, which is obviously derived from the fusing of the water droplets. Similar disordered microporous structures are observed with the concentration of DODA increasing from 0.25 mg/mL to 5 mg/mL. Thus, it is evident that DODA cannot stabilize the condensed water droplets efficiently. This result can be well explained from that the stability of molecules adsorbing at interface relates to the energy of removing the molecules from the interface, which dramatically decreases with decreasing the volume of the molecules [11,16]. Small surfactant molecules with low molecular weight adsorb/desorb at interface on a relatively fast timescale, making the interface unstable. Contrarily, the large sized SEC-1 with high molecular weight adsorbs at interface stably, which is thought to be irreversible due to the higher attaching energy in relation to the thermal energy, and thus can be used as the effective stabilizer. It has also been reported that the millimeter-sized water drops coated by nanosized particles show extremely high stability against coalescence, while in the case of surfactant-stabilized emulsions, this situation has never been realized [17]. Therefore, compared with small surfactant molecules, the larger sized SEC-1 is a good stabilizer for water droplets due to its strong adsorption at interface.

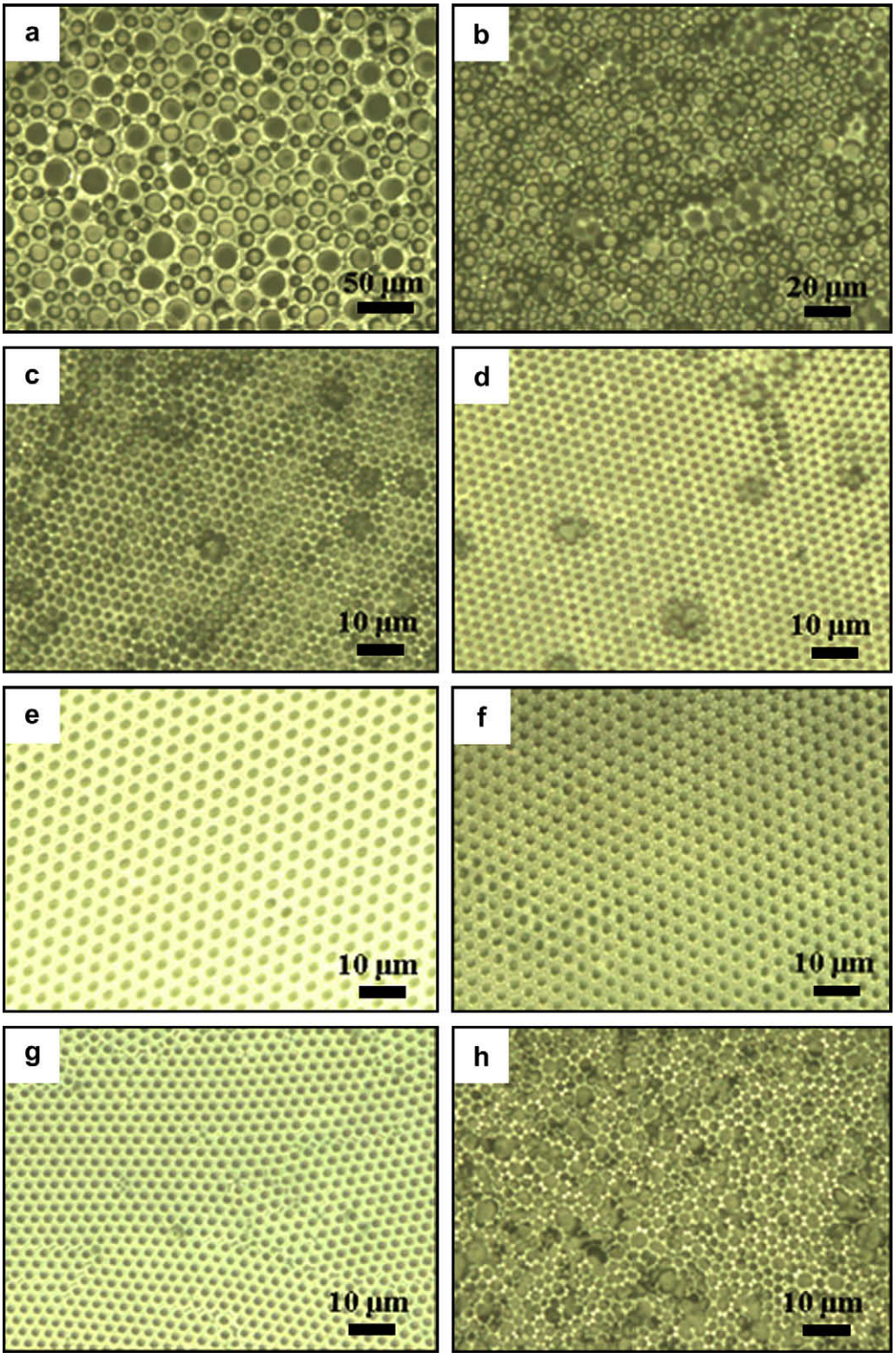

Fig. 2. Optical micrographs of patterned surfaces casting from 6 mg/mL of PS containing different concentrations of SEC-1: (a) 0.03 mg/mL, (b) 0.06 mg/mL, (c) 0.12 mg/mL, (d) 0.25 mg/mL, (e) 0.32 mg/mL (5 wt%), (f) 2 mg/mL, and (g) 6 mg/mL, respectively, as well as (h) 6 mg/mL of PS containing 1 mg/mL of DODA.

To further understand the organized structure of the honeycomb-patterned hybrid film, the film casting from the solution containing 6 mg/mL of PS and 1 mg/mL of SEC-1 was taken as an example for detailed observation through SEM and AFM. A close examination of the hybrid microporous film through SEM (Fig. 3a) shows that the holes are uniform and well ordered. And the holes appeared in the second layer are also highly ordered, which can be seen clearly through the surface layer (Fig. 3b). SEM image of cross-section (Fig. 3c) indicates that the holes are multilayered, and reach the bottom of the film. However, the holes are not open to the substrate, and the bottom of the film is sealed although the spacing between the holes and the surface of the substrate is very short. To

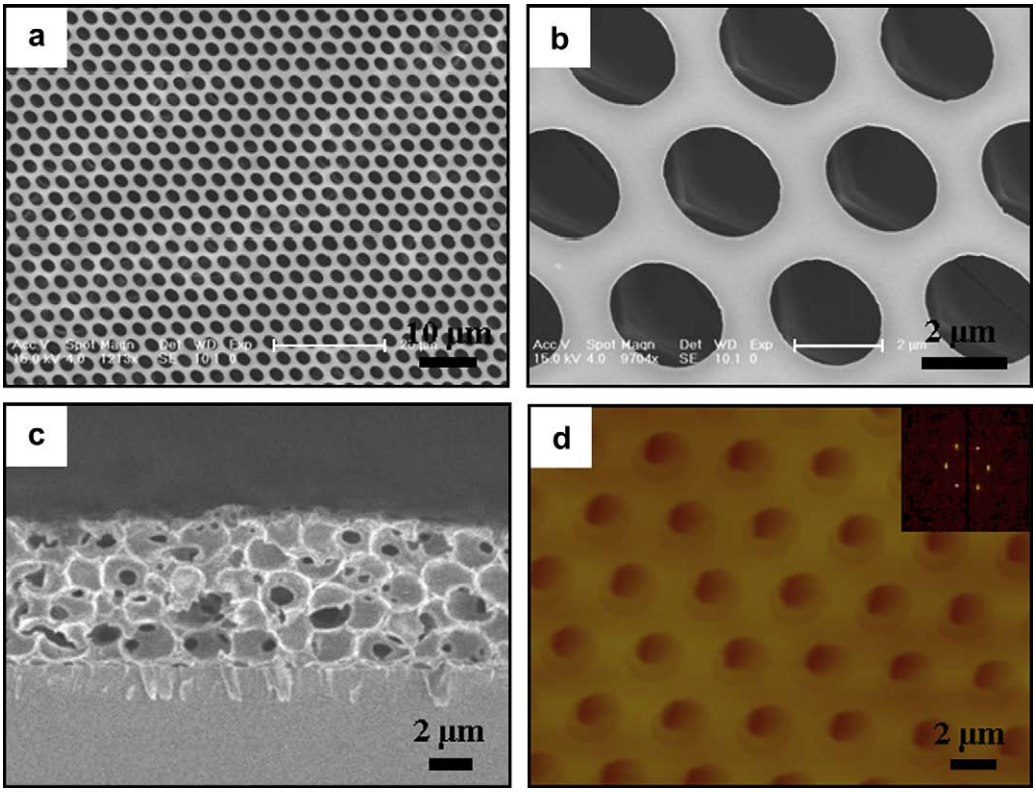

Fig. 3. Honeycomb structure images of the hybrid film casting from 6 mg/mL of PS containing 1 mg/mL of SEC-1: (a) SEM image of top surface, (b) the local magnification of (a), (c) SEM image of cross-section, and (d) AFM image and the corresponding FFT pattern (inset d).

identify whether the microporous structure passes through the whole film, we further evaluated the hybrid microporous film by peeling it from the substrate and observed a flat back surface without any holes, indicating that the bottom of the film is sealed and the water droplets cannot touch the substrate for the compact enveloping of SEC-1. In comparison with the microporous film of pure SEC-1, the hybrid microporous film we obtained in PS matrix exhibits a more ordered pattern on the surface and even in the inner of the film. The tapping mode AFM image further confirms the ordered micrometer-sized porous structure with a porous sublayer (Fig. 3d), where the average diameter of the surface holes is ca. 1800 nm separated by 800 nm. Fast Fourier Transform (FFT) pattern (Fig. 3d, inset) indicates a hexagonal arrangement of the holes in both the surface layer and the sublayer.

We further observed the morphology of the hybrid microporous film in a large area by decreasing the amplification of OM image, and found that it was difficult for the microporous film to keep order in the whole casting field, because grain boundaries separating ordered domains always exist on the film (Fig. S1). From the local magnified image of the boundary in the inset of Fig. S1, it can be clearly seen that the irregular borders divide the ordered arrangements of the holes with different orientations into separated domains. These irregular borders are derived from the collision of ordered arranged water droplet domains during the final stage of solvent evaporation, and such a phenomenon is universal and unavoidable in the formation of breath figure patterns [18]. Noticeably, in a single domain the array of the holes is highly ordered, and the order only breaks down at the domain border.

3.2. Self-assembling of SEC-1 in PS microporous film

In the case of breath figure formation from a polymer/SEC-1 solution, accompanied with the self-organization of the condensed water droplets, the interface between solution and water droplets could serve as the template for SEC-1 assembling. On the evaporation of the solvent and the water droplets, spherical holes remain and SEC-1 is locked within the holes. Thus, SEC-1 should accumulate on the internal surfaces of the holes after the solidification of hybrid microporous film. By employing TEM, we can directly observe the interfacial segregation of SEC-1 to the internal surfaces of the holes through the heavy metal tungsten ions containing in SEC-1. Since the electron beam is difficult to penetrate a thick microporous film for the high tungsten content, we decreased the concentration of the mixed casting solution to 0.5 mg/mL for PS and 0.083 mg/mL for SEC-1 in a constant ratio of 6:1 as we employed above, and prepared the film under a relatively low humid condition in order to obtain a discrete hole structure for clear observation. From the image in Fig. 4, evident black rings resulting from the accumulation of SEC-1 along the edges of the holes are observed on the thin film, and surely, there are still some SEC-1s dispersing in the film. This result directly confirms the self-assembling of SEC-1 at the PS solution–water droplet interface during the breath figure formation. In the case of ordered microporous film prepared under the relatively high concentration and humidity, the segregation of SEC-1 on the internal surfaces of the holes should be the same, and was further demonstrated by TEM performed on the thin cross-section of the ordered microporous film. The black line clearly appears at the film–air interface of the hole, which is evidently attributed to the assembling of SEC-1 at the PS solution–water droplet interface, as seen in the Supporting information. Unfortunately, the figure of the hybrid microporous film has not been well kept because of the breakage to the film during the preparation of super thin slice for a cross-sectional view of the hybrid structure.

It is known that amphiphilic SECs tend to self-assemble into lamellar structures in solid, thin film, and even in solution through the organization driven by hydrophobic force [19]. To determine

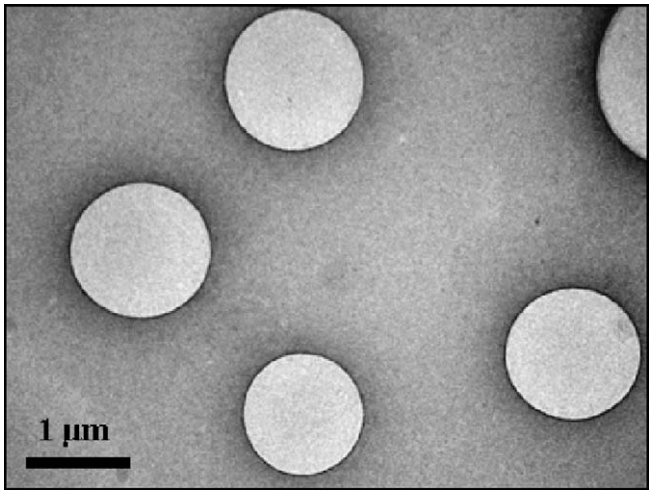

Fig. 4. TEM image of the hybrid film casting from 0.5 mg/mL of PS containing 0.083 mg/mL of SEC-1 under the relatively low humid condition.

the aggregated structure of SEC-1 on the internal surfaces of the holes, the microporous film was characterized by X-ray diffraction, as seen in Fig. 5. Three sharp Bragg diffraction peaks appear at 2.78° (001), 5.51° (002), and 8.26° (003), suggesting a well ordered lamellar structure with a layer spacing of 3.2 nm. And, the layer spacing is similar to the value of the previously reported SEC-1 solid [20]. Considering that the ideal diameter of SEC-1 is 4.7 nm, the alkyl chains of SEC-1 in the microporous film should be in an almost fully interdigitated structure with the interdigitated length of 1.5 nm, suggesting the tight packing of SEC-1. Moreover, the common solvent-casting film of SEC-1 doped PS solution also shows a similar lamellar structure, deriving from the aggregation of SEC-1 in PS due to their incompatibility during the evaporation of chloroform. And in contrast to the common casting film, the Bragg diffractions of the honeycomb-patterned film exhibit higher intensity and narrower full-width at half-maximum. This suggests that the condensed water droplets serve as the template for SEC-1 self-assembling into a more ordered lamellar structure with tight packing at the PS solution–water droplet interface and meanwhile the accumulation of SEC-1 around the water droplets stabilizes the water droplets much more efficiently, which largely enhances the order of the hybrid microporous film.

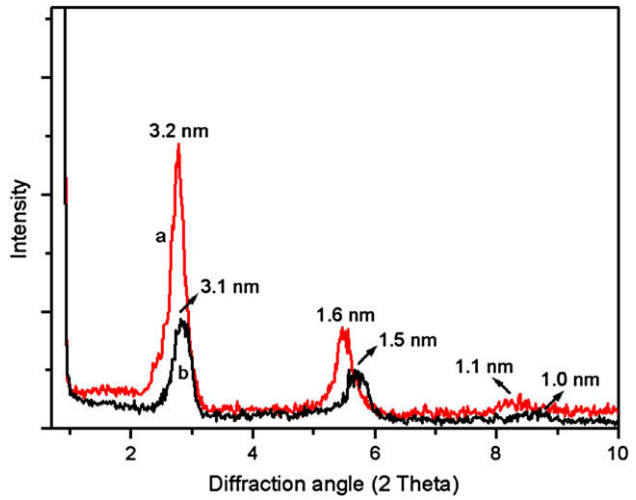

Fig. 5. X-ray diffraction patterns of the hybrid film casting from 6 mg/mL of PS containing 1 mg/mL of SEC-1 in the low angle region under (a) the humid condition and (b) laboratory condition (relatively dry condition).

Based on above data and the similar self-assembling behavior of CdSe nanoparticles at the polymer solution–water droplet interface, reported in the literature, we propose a model to understand the formation process of SEC-1 functionalized breath figure holes. Fig. 6 describes the cross-sectional schematic drawing of SEC-1 self-assembling at a water droplet–PS solution interface during the breath figure formation [12b]. Accompanied with solvent evaporation and the self-organization of water droplets, amphiphilic SEC-1 segregates to the PS solution–water droplet interface and stabilizes water droplets. DODA component that binds on POM-1 electrostatically in SEC-1 rearranges at the PS solution–water droplet interface and departs from the aqueous subphase driven by hydrophobic force. Such an uneven distribution of DODA part at air–water interface has been reported in our previous study for another SEC, $(DODA)_{16}AsW_{30}Cu_4O_{112}$, and we have further demonstrated

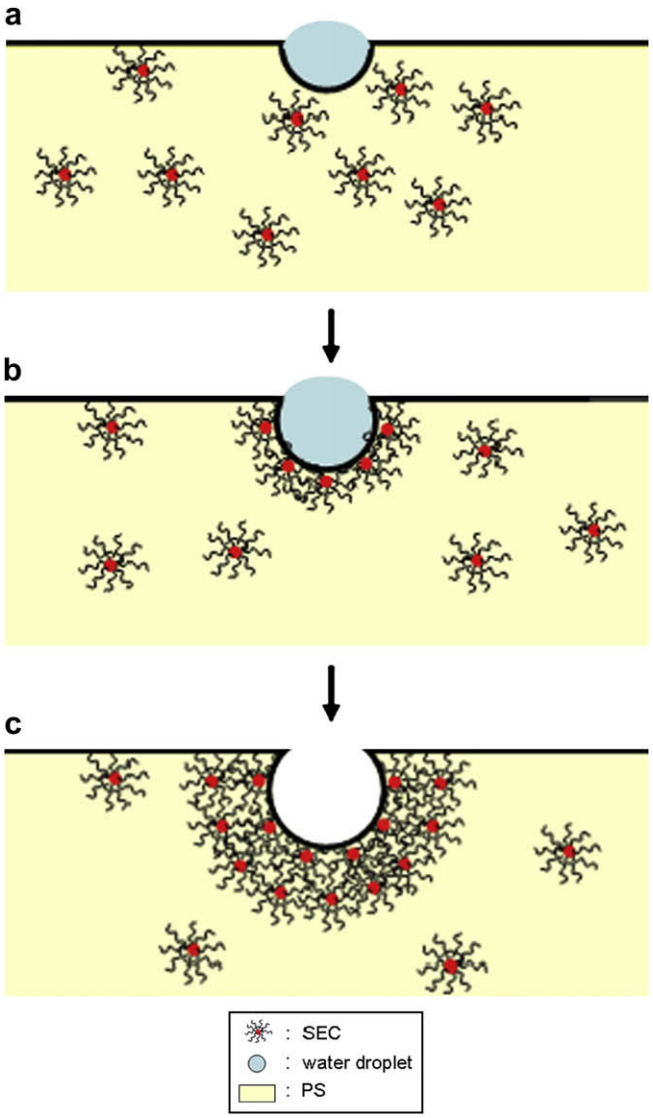

Fig. 6. The cross-sectional schematic drawing of SEC-1 self-assembling at a water droplet–PS solution interface during the breath figure formation: (a) a small water droplet condenses onto the solution surface, (b) the water droplet grows by molecular condensation and sinks into the PS solution while SEC-1 segregates to the PS solution–water droplet interface, and subsequently, templated by the SEC-1 segregated at the interface, SEC-1 in the solution continues transferring to the interface and self-assembles into an ordered and tight lamellar structure, and (c) after the completely evaporation of chloroform and water, SEC-1 is accumulated on the internal surface of the hole with the ordered and tight lamellar structure.

that the rearrangement of DODA electrostatically attached on POM surface is feasible in solution from both theoretical and experimental aspects [19]. Subsequently, templated by those SEC-1 segregating at the interface, other SEC-1 in bulk continues transferring to the interface and self-assembles into an ordered and tight lamellar structure, which makes the condensed water droplets more stable. This compact interface layer efficient enwraps the water droplets and makes them separate from each other. The model can be evidently supported by the fact that the water droplets at the bottom of the thin film are still separated and non-contactable to the substrate, as observed from SEM image of cross-section. At last, after both organic solvent and water droplets evaporate completely, highly ordered honeycomb-patterned hybrid PS film forms with SEC-1 accumulating on the internal surfaces of the holes in an ordered and tight lamellar structure. Therefore, we could obtain SEC-1 functionalized breath figure holes in PS matrix via a straightforward, one-step process combining the self-organized and self-assembly processes on different length scales by doping SEC-1 into PS solution. And on the top layers of the internal surfaces of the holes, SEC-1 accumulates in a distorted and reorganized state due to phase separation, which is favorable for the better performance of the function of POM-1.

3.3. Luminescent properties

As POM-1 is an inorganic cluster of europium-substituted polyoxotungstate, the PS microporous film in which the holes are functionalized with SEC-1 should exhibit intense red emission and is expected to be promising luminescent material. In the present investigation, the luminescence of POM-1 is indeed found well retained in the hybrid microporous film, as has been proved in PMMA and SiO_2 hybrids [14d,14e]. The emission spectrum excited at the O → W LMCT band (275 nm) shows the characteristic $^5D_0 \rightarrow {}^7F_j$ ($j = 0, 1, 2, 3, 4$) transitions of Eu^{3+}, as shown in Fig. 7. The intensity ratio of $^5D_0 \rightarrow {}^7F_2$ transition to $^5D_0 \rightarrow {}^7F_1$ transition is often applied to evaluate the variation of Eu^{3+} symmetry under different conditions, and an increase in its value always corresponds to a decrease of Eu^{3+} symmetry [21]. Our results show that the symmetry of Eu^{3+} decreases in the hybrid microporous film, compared with pure POM-1, SEC-1 and even the common casting hybrid film, indicating the uneven distribution of DODA cations and POM-1 anion of SEC-1 on the internal surfaces of the holes. Similar result is also observed in the film of pure SEC-1 [14d,22].

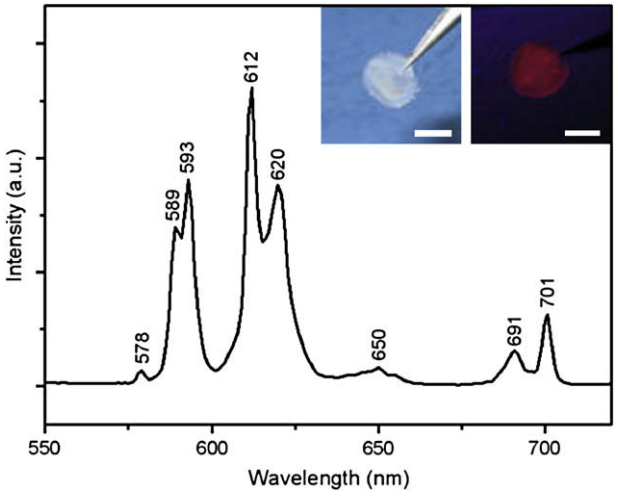

Fig. 7. The emission spectrum of the hybrid microporous film at room temperature (ex: 275 nm), and the digital photographs of the hybrid microporous film in daylight (left) and in ultraviolet light (right) (inset) (scale bar is 1 cm long).

$$k_r = k_{r(0\rightarrow 1)} \frac{\sum_{j=0}^{4} S_{(0\rightarrow j)}}{S_{(0\rightarrow 1)}} \quad (1)$$

$$k_{\text{tot}} = \frac{1}{\tau} = k_r + k_{\text{nr}} \quad (2)$$

$$\eta = \frac{k_r}{k_r + k_{\text{nr}}} \quad (3)$$

Because $^5D_0 \rightarrow {}^7F_1$ transition is a magnetic dipole transition and its intensity is invariable with the microenvironment of Eu^{3+}, we can use it as a reference for the calculation of luminescent quantum yield. Based on the intensity parameters of the Eu^{3+} emission spectrum, the total radiative rate of $^5D_0$ can be calculated by Eq. (1), where $k_{r(0\rightarrow 1)}$ is the radiative rate constant of $^5D_0 \rightarrow {}^7F_1$ transition and its value has been reported to be $1.35 \times 10^2\ s^{-1}$, $S_{(0\rightarrow j)}$ and $S_{(0\rightarrow 1)}$ are the integral intensities of the $^5D_0 \rightarrow {}^7F_j$ and $^5D_0 \rightarrow {}^7F_1$ transitions, respectively [23]. All the $^5D_0$ decay curves fit well to a single-exponential function, and the fitted lifetimes (τ) are shown in Table 1. Based on these data, the total decay rate of $^5D_0$ (k_{tot}) can be estimated from Eq. (2). Finally, the absolute emission quantum yield, η, is determined by Eq. (3). All the deduced fluorescent data of Eu^{3+} in different environments are summarized in Table 1. These results suggest that the η of POM-1 keeps well in the hybrid microporous film, which is similar with that in the common casting hybrid film. Furthermore, the hybrid microporous film contributes higher η than the microporous film casting from pure SEC-1, indicating that the polymer matrix is advantageous to gain a higher luminescence efficiency, which is consistent with our previous report [14d].

3.4. Incorporation of Ag and Fe_2O_3 nanoparticles

SECs with other diverse properties could also be introduced into the internal surfaces of the holes of the PS microporous film in this way. And on the basis of the obtained SECs decorated hybrid microporous film, we could construct further functionalized pattern with specific property according to the different purposes. As one example, we have introduced $(DOAH)_{12}[EuP_5W_{30}O_{110}]$ (SEC-2) (DOAH: dioctadecylammonium hydrobromide) to the internal surfaces of the holes of the PS microporous film. The POM of which exhibits strong photochromic and redox ability [14g,24], and thus, with this cluster, POM-2, we could realize the in-situ synthesis of metal nanoparticles in the holes of the film. First, the prepared SEC-2 functionalized PS microporous film was irradiated by UV light for 20 min to get the reduced POM-2, which could be treated as the reductant. Then the film was dipped into a 0.1 M of $AgNO_3$ deaerated aqueous solution for 48 h, and Ag nanoparticles were obtained through the reduction of silver ions. As shown in Fig. 8a, well dispersed Ag nanoparticles with regular spherical morphology in a narrow size distribution (40 nm in average diameter) were successfully in-situ prepared in the holes of the PS film, and the microporous structure was still well retained. In comparison with the patterns directly prepared by pure organic modified Au or Ag

Table 1
Summary of experimental $^5D_0$ lifetime τ, calculated decay rate k_{tot}, radiative rate k_r, nonradiative rate k_{nr}, and absolute quantum yield η.

Sample	$I_{(0\rightarrow 2)}/I_{(0\rightarrow 1)}$	τ [ms]	k_{tot} [ms^{-1}]	k_r [ms^{-1}]	k_{nr} [ms^{-1}]	η [%]
POM-1 [13a]	0.367	2.80	0.36	0.27	0.09	75.6
SEC-1 (common casting film)	0.770	1.33	0.7519	0.4337	0.3182	57.7
SEC-1 (microporous film)	1.076	1.30	0.7692	0.4468	0.3224	58.1
PS/SEC-1 (common casting film)	1.250	1.35	0.7407	0.4669	0.2738	63.0
PS/SEC-1 (microporous film)	1.448	1.30	0.7692	0.4932	0.2760	64.1

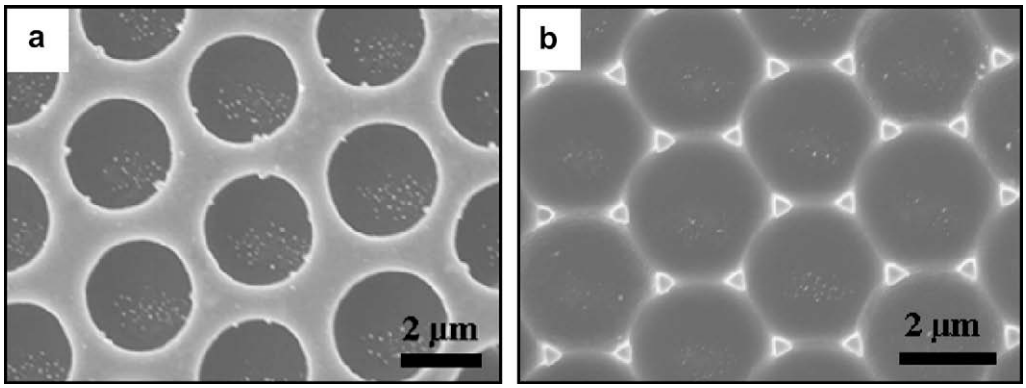

Fig. 8. SEM image of the hybrid microporous film containing Ag nanoparticles (a) before and (b) after the removal of the surface of the film using adhesive tape.

nanoparticles, the present SECs doped PS film seems more effective in gathering the nanoparticles in the holes of the film. Of course, due to the small amount of SEC-2 remaining on other places of the film surface or the move of Ag nanoparticles, some Ag nanoparticles appeared avoidlessly on the top surface of the microporous film other than in the holes. In spite of this, the present strategy provides a facile route for the preparation of multicomponent patterned films. Apparently, the selected growth of silver nanoparticles on the microporous film can be attributed to the patterned aggregation of SECs. Furthermore, a pincushion-like microporous structure with Ag nanoparticles in the holes was obtained through peeling off the surface using adhesive tape (Fig. 8b). By varying the dipping solution, Au, Pd, Pb etc. nanoparticles could also be facilely synthesized via the similar procedure [25].

In addition to the patterned surfaces of gold and silver nanoparticles, the patterned film containing magnetic nanoparticles is also limited [26]. As we know, normally only some polymers and surface modified nanoparticles with proper amphiphilicity could form ordered microporous structure by themselves. Thus, it is a challenge to seek a facile method to introduce various substances with specific properties to the ordered microporous structures, and to execute their functions in the film. SEC-1 doped PS solution owns both the stability to the condensed water droplets and the processibility, which may be applied to induce other functional substances to form microporous structure through the addition of the extra component. Therefore, the present hybrid matrix provides a possibility to prepare magnetic patterned structure by employing organic modified magnetic nanoparticles. We have prepared octylamine-protected Fe_2O_3 nanoparticles (average diameter: 5.7 nm), and tried to prepare magnetic microporous structure via breath figures. It should be noted that we did not obtain any ordered morphology besides some irregular aggregates by using Fe_2O_3 nanoparticles alone (1 mg/mL), as shown in Fig. 9a. To support the formation of magnetic microporous structure, the

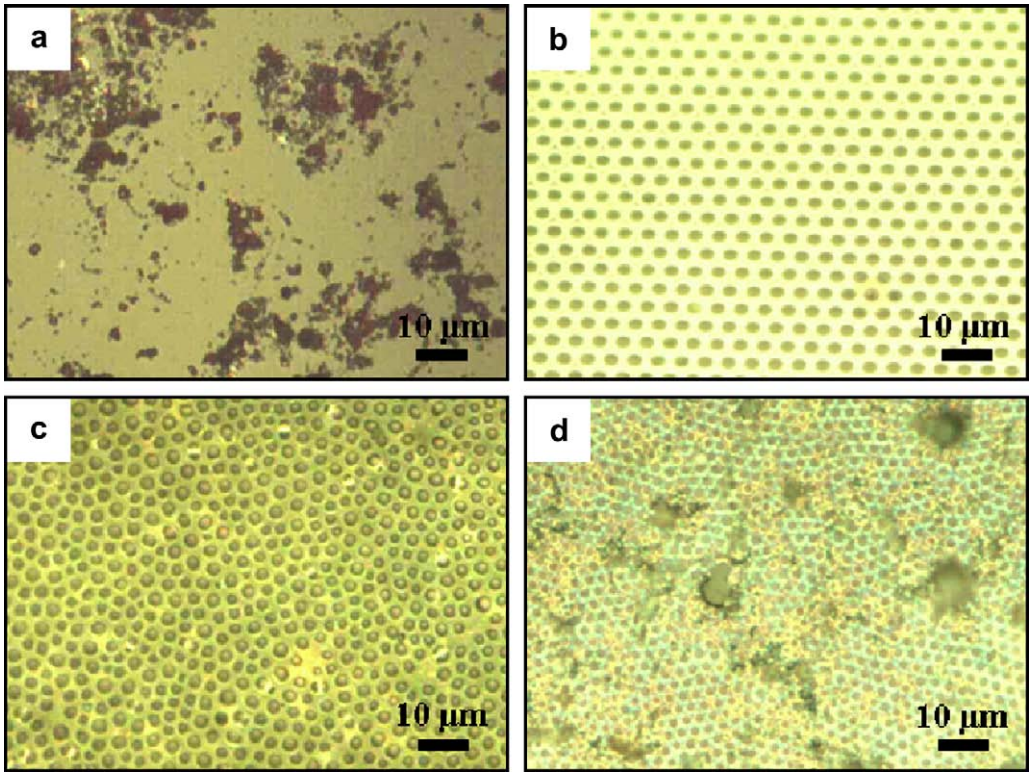

Fig. 9. Optical micrographs of patterned surfaces casting from (a) 1 mg/mL of Fe_2O_3 nanoparticle, (b) 6 mg/mL of PS containing 1 mg/mL of Fe_2O_3 nanoparticle, (c) 5 mg/mL of SEC-1 containing 1 mg/mL of Fe_2O_3 nanoparticle, and (d) 6 mg/mL of PS containing both 1 mg/mL of Fe_2O_3 nanoparticle and 1 mg/mL of SEC-1, respectively.

Fe_2O_3 nanoparticles were added to the mixed solution of SEC-1 and PS for breath figures (6 mg/mL of PS containing 1 mg/mL of Fe_2O_3 nanoparticle and 1 mg/mL of SEC-1). As expected, the highly ordered microporous structure forms in a large area (Fig. 9b). The doped Fe_2O_3 nanoparticles did not affect the order of the hybrid film, and the magnetism of the Fe_2O_3 nanoparticles is remained in the microporous structure as shown in the MFM image (see Supporting information). As SEC-1 is luminescent due to the existence of Eu in its POM, the prepared highly ordered microporous film shows intense red emission under ultraviolet light excitation, and could be easily magnetized by the magnet (see Supporting information). It should be emphasized that the SEC-1 doped PS matrix is unique for constructing the magnetic patterned surface. We have also tried doping Fe_2O_3 nanoparticles with PS and SEC-1, respectively. However, only poor ordered structure with irregular shaped holes is observed when casting the Fe_2O_3 nanoparticle doped PS solution (6 mg/mL of PS containing 1 mg/mL of Fe_2O_3 nanoparticle), as seen in Fig. 9c. As to the case of Fe_2O_3 nanoparticle mixed SEC-1 solution (5 mg/mL of SEC-1 containing 1 mg/mL of Fe_2O_3 nanoparticle), uncontinuous ordered structure forms for the poor processibility of the mixture, as illustrated in Fig. 9d. Therefore, we believe that it is the synergetic effect of SEC-1 and PS that makes the mixed film be an appropriate matrix for the formation of ordered microporous structure containing these kind of magnetic nanoparticles. The present results imply that other molecules or nanoparticles with various functions could also be introduced into the microporous structure via the same method.

4. Conclusion

We have demonstrated the use of SEC-1 to functionalize the breath figure holes in PS film in a straightforward, one-step process through the site-controlled self-assembling of SEC-1 in PS film. Accompanied with the self-organization of the water droplets, amphiphilic SEC-1 can segregate to the PS solution–water droplet interface to stabilize the water droplets and self-assemble into an ordered and tight lamellar structure around the water droplets. And the doped SEC-1 effectively enhances the order of the PS microporous film, forming highly ordered hybrid microporous structure in a large scale. In the hybrid microporous film, the internal surfaces of the holes are functionalized with SEC-1, and not only ordered microporous structure of PS but also ordered microarrays of SEC-1 functionalized holes with an ordered lamellar structure in PS matrix are obtained. The formed highly ordered honeycomb-patterned hybrid film shows intense red emission in ultraviolet light and can be worked as the self-supporting film owing to the well maintenance of the original fluorescence of SEC-1 and the good processibility of PS. Furthermore, on the basis of the obtained SECs functionalized PS microporous film, metal and magnetic nanoparticles have been successfully introduced into the microporous structure, respectively, by adopting suitable ways. The present investigation proves a convenient way to fabricate highly ordered microarrays of SEC-1 functionalized holes in PS matrix, combining the self-organized and self-assembly processes on different length scales. We are delighted to see that the present method could also be extended to other polymers such as PMMA (see Supporting information). And, we believe that POMs with a variety of applicable properties could be readily applied to functionalize the holes in polymer microporous films, which opens up potential applications in sensor, separation and catalysis.

Acknowledgments

The authors acknowledge the financial support from National Basic Research Program (2007CB808003), National Natural Science Foundation of China (20574030, 20731160002), PCSIRT of Ministry of Education of China (IRT0422), and Open Project of State Key Laboratory of Polymer Physics and Chemistry of CAS. We thank Professor F. Schue from University of Montpelier for the helpful discussion on the occasion of his visiting us, supported by 111 Project (B06009).

Appendix. Supporting information

Supplementary data associated with this article can be found in the online version at doi: 10.1016/j.polymer.2009.02.036.

References

[1] (a) Tanev PT, Chibwe M, Pinnavaia TJ. Nature 1994;368:321–3;
(b) Jiang P, Hwang KS, Mittleman DM, Bertone JF, Colvin VL. J Am Chem Soc 1999;121:11630–7;
(c) Wijnhoven JEGJ, Vos WL. Science 1998;281:802–4;
(d) Hulteen JC, Jirage KB, Martin CR. J Am Chem Soc 1998;120:6603–4.
[2] (a) Widawski G, Rawiso M, Francois B. Nature 1994;369:387–9;
(b) Francois B, Pitois O, Francois J. Adv Mater 1995;7:1041–4.
[3] (a) Srinivasarao M, Collings D, Philips A, Patel S. Science 2001;292:79–83;
(b) Bunz UHF. Adv Mater 2006;18:973–89;
(c) Karthaus O, Maruyama N, Cieren X, Shimomura M, Hasegawa H, Hashimoto T. Langmuir 2000;16:6071–6;
(d) Pitois O, Francois B. Eur Phys J B 1999;8:225–31;
(e) Maruyama N, Koito T, Nishida J, Sawadaishi T, Cieren X, Ijiro K, et al. Thin Solid Films 1998;327–329:854–6.
[4] Peng J, Han YC, Fu J, Yang YM, Li BY. Macromol Chem Phys 2003;204:125–30.
[5] Stenzel-Rosenbaum MH, Davis TP, Fane AG, Chen V. Angew Chem Int Ed 2001;40:3428–32.
[6] (a) Cheng CX, Tian Y, Shi YQ, Tang RP, Xi F. Langmuir 2005;21:6576–81;
(b) Hayakawa T, Horiuchi S. Angew Chem Int Ed 2003;42:2285–9.
[7] (a) Nishikawa T, Ookura R, Nishida J, Arai K, Hayashi J, Kurono N, et al. Langmuir 2002;18:5734–40;
(b) Yu CL, Zhai J, Gao XF, Wan MX, Jiang L, Li TJ, et al. J Phys Chem B 2004;108:4586–9.
[8] (a) Govor LV, Bashmakov IA, Kiebooms R, Dyakonov V, Parisi J. Adv Mater 2001;13:588–91;
(b) Song LL, Bly RK, Wilson JN, Bakbak S, Park JO, Srinivasarao M, et al. Adv Mater 2004;16:115–8;
(c) Vamvounis G, Nyström D, Antoni P, Lindgren M, Holdcroft S, Hult A. Langmuir 2006;22:3959–61.
[9] (a) Yonezawa T, Onoue SY, Kimizuka N. Adv Mater 2001;13:140–2;
(b) Shah PS, Sigman MB, Stowell CA, Lim KT, Johnston KP, Korgel BA. Adv Mater 2003;15:971–4;
(c) Li J, Peng J, Huang WH, Wu Y, Fu J, Cong Y, et al. Langmuir 2005;21:2017–21.
[10] (a) Peng J, Han YC, Yang YM, Li BY. Polymer 2004;45:447–52;
(b) Bolognesi A, Mercogliano C, Yunus S, Civardi M, Comoretto D, Turturro A. Langmuir 2005;21:3480–5.
[11] (a) Binks BP. Curr Opin Colloid Interface Sci 2002;7:21–41;
(b) Binder WH. Angew Chem Int Ed 2005;44:2–5;
(c) Wang D, Duan H, Möhwald H. Soft Matter 2005;1:412–6.
[12] (a) Zhang Y, Wang C. Adv Mater 2007;19:913–6;
(b) Böker A, Lin Y, Chiapperini K, Horowitz R, Thompson M, Carreon V, et al. Nat Mater 2004;3:302–6;
(c) Saunders AE, Shah PS, Sigman MB, Hanrath T, Hwang HS, Lim KT, et al. Nano Lett 2004;4:1943–8;
(d) Hayakawa T, Yokoyama H. Langmuir 2005;21:10288–91;
(e) Stenzel MH, Davis TP. Aust J Chem 2003;56:1035–8;
(f) Nygard A, Davis TP, Barner-Kowollik C, Stenzel MH. Aust J Chem 2005;58:595–9;
(g) Barner-Kowollik C, Dalton H, Davis TP, Stenzel MH. Angew Chem Int Ed 2003;42:3664–8;
(h) Sun W, Ji J, Shen JC. Langmuir la8024217.
[13] (a) Pope MT, Müller A. Angew Chem Int Ed 1991;30:34–48;
(b) Chem Rev 1998;98:1. The entire issue is devoted to polyoxometalates.
[14] (a) Bu WF, Wu LX, Hou XL, Fan HL, Hu CW, Zhang X. J Colloid Interface Sci 2002;251:120–4;
(b) Bu WF, Li W, Li HL, Wu LX, Tang AC. J Colloid Interface Sci 2004;274:200–3;
(c) Bu WF, Wu LX, Tang AC. J Colloid Interface Sci 2004;269:472–5;
(d) Li HL, Qi W, Li W, Sun H, Bu WF, Wu LX. Adv Mater 2005;17:2688–92;
(e) Qi W, Li HL. Adv Mater 2007;19:1983–7;
(f) Sugeta M, Yamase T. Bull Chem Soc Jpn 1993;66:444–9;
(g) Creaser I, Heckel MC, Neitz RJ, Pope MT. Inorg Chem 1993;32:1573–8.
[15] (a) Bu WF, Li HL, Sun H, Yin SY, Wu L. J Am Chem Soc 2005;127:8016–7;
(b) Sun H, Li HL, Bu WF, Xu M, Wu LX. J Phys Chem B 2006;110:24847–54.
[16] Chattopadhyay AK, Shah DO, Ghaicha L. Langmuir 1992;8:27–30.
[17] Zhai X, Efrima S. J Phys Chem 1996;100:11019–28.

[18] (a) Tian Y, Ding HY, Jiao QZ, Shi YQ. Macromol Chem Phys 2006;207:545–53;
(b) Xu Y, Zhu BK, Xu YY. Polymer 2005;46:713–7.
[19] (a) Bu WF, Fan HL, Wu LX, Hou XL, Hu CW, Zhang G, et al. Langmuir 2002;18:6398–403;
(b) Bu WF, Wu LX, Zhang X, Tang AC. J Phys Chem B 2003;107:13425–31;
(c) Li HL, Sun H, Qi W, Xu M, Wu LX. Angew Chem Int Ed 2007;46:1300–3.
[20] Bu WF, Li HL, Li W, Wu LX, Zhai CX, Wu YQ. J Phys Chem B 2004;108:12776–82.
[21] (a) Nogami M, Abe Y. J Non-Cryst Solids 1996;197:73–8;
(b) Capobianco JA, Proulx PP, Bettinelli M, Negrisolo F. Phys Rev B 1990;42:5936–44.
[22] Zhang TR, Spitz C, Antonietti M, Faul CFJ. Chem Eur J 2005;11:1001–9.
[23] (a) Yamase T, Kobayashi T, Sugeta M, Naruke H. J Phys Chem A 1997;101:5046–53;
(b) Carlos LD, Messadeq Y, Brito HF, Sa-Ferreira RA, Bermudz V, Ribeiro SJL. Adv Mater 2000;12:594–8.
[24] (a) Mandal S, Selvakannan PR, Pasricha R, Sastry M. J Am Chem Soc 2003;125:8440–1;
(b) Qi W, Li HL, Wu LX. J Phys Chem B 2008;112:8257–63.
[25] Troupis A, Hiskia A, Papaconstantinou E. Angew Chem Int Ed 2002;41:1911–4.
[26] Bashmakov IA, Govor LV, Solovieva LV, Parisi J. Macromol Chem Phys 2002;203:544–9.